Proceedings of the 21st ICSMGE, Vienna, Austria, 14 – 19 June 2026. Pistrol, Adam & Schweiger (eds.)
Published by: ÖGG, Austrian Society for Geomechanics, Salzburg, Austria, ISBN 978-3-9503898-4-5
https://doi.org/10.53243/ICSMGE2026-2162

The Importance of Unloading in Modelling Drained Cone Penetration Test

Xingyi Wu
Department of Civil and Mining Engineering, University of Toronto, Toronto, Canada
Department of Infrastructure Engineering, The University of Melbourne, Melbourne, Australia

Mason Ghafghazi
Department of Civil and Mining Engineering, University of Toronto, Toronto, Canada, mason.ghafghazi@utoronto.ca

Yinghui Tian, Shiaohuey Chow
Department of Infrastructure Engineering, The University of Melbourne, Melbourne, Australia

João Paulo de Sousa Silva
Vale S.A., Santa Luzia, Minas Gerais, Brazil

ABSTRACT: The cone penetration test (CPT) is the primary site characterization tool in geotechnical engineering. In-soil measurements and models of cone penetrations have suggested that unloading is the predominant behaviour mode of the soil past the cone tip. This behaviour mode affects the friction sleeve and the tip resistance in drained penetration simulations, and can potentially affect conventionally measured pore water pressures at the cone shoulder in partially drained CPT simulations. With a need for better interpretation of the CPT in non-conventional soils such as mine tailings, numerical modelling of the cone penetration process is gaining more popularity. At the same time, progress in computational power is making more realistic models feasible. This paper expands on previous work on modelling drained cone penetration in sand using the popular critical state constitutive model NorSand implemented in ABAQUS and utilizing Arbitrary Lagrangian Eulerian (ALE) formulation. NorSand's internal cap was implemented into the user material subroutine (UMAT) for Abaqus/Standard. The cap formulations were clarified and expanded, and objective criteria were set up to differentiate unloading from softening. The implementation was validated by simulating triaxial compression loading-unloading tests. The drained cone penetration model was then extended to include cap unloading. The tip resistance and the sleeve friction with the internal cap were compared with that from NorSand without the internal cap. The comparison showed that the inclusion of the internal cap can reduce sleeve friction and slightly increase tip resistance.

KEYWORDS: Cone Penetration Test, finite element analysis, NorSand, large deformation analysis, unloading.

1 INTRODUCTION

The Cone Penetration Test (CPT) is one of the most widely used in-situ tests in geotechnical engineering. During cone penetration, three measurements are commonly obtained: tip resistance q_c, sleeve friction f_s, and pore water pressure u_2. These measurements can be interpretated to determine subsurface stratigraphy and estimate the engineering properties of soils. A good interpretation method relies on the deep understanding soil response during penetration. Liu et al. (2025) placed strain and stress sensors within a sand sample in a CPT calibration chamber to measure the changes in strain and stress as the cone approached and passed the sensors. Their results showed that the soil response during penetration can generally be divided into two stages: loading until cone tip arrives and unloading when cone tip and shoulder pass. Therefore, both loading and unloading stress paths matter in modelling the CPT.

Numerical modelling is a powerful tool to understand and analyze the CPT and has been conducted through different methods, such as cavity expansion (e.g., Yu and Houlsby 1991, Ghafghazi and Shuttle 2008), finite element method (FEM) (e.g., Yi et al. 2012, Moug et al. 2019, Mozaffari and Ghafghazi 2023a), material point method (MPM) (e.g., Ayala et al. 2023, Martinelli et al. 2024), among others. However, in these simulations, the unloading stress path behind the cone has not received much attention. Cavity expansion method is by definition a one-way loading process. The cone is explicitly simulated in the FEM, and MPM. In these simulations, the constitutive models used were Modified Cam Clay and Tresca for clay, and Mohr-Coulomb and Druck-Prager models for sand. When soil is unloaded, the behaviour is elastic in these models. The elastic assumption is not realistic for granular soils. Therefore, a constitutive model that is able to capture unloading behaviour well is necessary for CPT simulations.

NorSand is a critical state based model for cohesionless soils, originally proposed by Jefferies (1993). NorSand has a bullet-shaped yield surface similar to Cam Clay's. NorSand can simulate the general loading stress path very well, for example, triaxial compression test (e.g., Mozaffari et al., 2022), uplift capacity of plate anchor in sand (e.g., Liu et al. 2024), tip resistance of CPT (e.g., Mozaffari and Ghafghazi 2023). NorSand's original bullet-shaped yield surface produces a purely elastic response in unloading. To solve this issue, Jefferies (1997) defined a straight vertical line at the maximum dilatancy mean stress, referred to as the 'internal cap'. If a stress path crosses the internal cap, it causes plastic strain. Dabeet (2008) used it to simulate unloading in triaxial compression tests and showed that the internal cap in NorSand can simulate soil response in unloading well.

In this paper, NorSand was implemented into an Abaqus/Standard UMAT subroutine, with its internal cap. This necessitated formulating new criteria to differentiate unloading from softening for application in boundary value problems. The UMAT was used to simulate the triaxial compression load-unload-reload tests. The comparison between simulation results and experimental data demonstrates NorSand's capabilities in simulating unloading behaviour. Two existing CPT chamber tests were simulated to study the effect of unloading on CPT measurements, by using NorSand without the internal cap and NorSand with the internal cap. The inclusion of internal cap can increase tip resistance and decrease sleeve friction such that the simulations have a better comparison with chamber test data. The stress paths from the two cases showed that inclusion of the internal cap can turn the unloading path from an elastic to a plastic process demonstrating softening behaviour.

2 CONSTITUTIVE MODEL IMPLEMENTATION

2.1 *NorSand with the internal cap*

NorSand, initially created by Jefferies (1993), is a critical state based Cambridge-type constitutive model for sand. The yield surface is derived in a similar way to the Cam Clay by using the normality and dilatancy definition. This approach produces a bullet-shaped yield surface. Different from the unique normal consolidation line (NCL) in clay, an infinity of NCLs exists for granular soils. This characteristic requires the yield surface to be decoupled from the critical state line (CSL). Figure 1 shows the yield surface of NorSand. The apex of the bullet is defined as image state. To achieve the mentioned decoupling, the stress ratio at image state, M_i, is not always equal to the stress ratio at critical state, M. The image state converges to the critical state with shear strain, making M_i eventually equal to M. This yield surface's efficiency has been proven for simulating many loading stress paths, for example, triaxial compression tests (e.g., Mozaffari et al., 2022) and direct simple shear test (e.g., Handspiker and Ghafghazi 2024). However, when the soil is unloaded (inward stress paths relative to the yield surface), the response is purely elastic and always produces elastic strains, which is not realistic soil behaviour, especially for granular soils.

To address this, an internal cap was defined by Jefferies (1997). Experimental results showed a maximum dilatancy exists for cohesionless soils and it depends on the stress state of the soil. As shown in Figure 1, the maximum dilatancy occurs to the left of the image state for dense soils, and to the right of the image state for loose soils. The internal cap was defined as a vertical straight line at the position of maximum dilatancy by Jefferies (1997). When stress paths cross the internal cap, they can produce plastic responses instead of elastic. The internal cap is represented by Equation (1).

$$p'_{cap} = p'_i e^{\frac{\chi_i \psi_i}{M_{i,tc}}} \tag{1}$$

where p'_{cap} and p'_i are mean stresses at the internal cap and image state, respectively. ψ_i is the state parameter at the image state, calculated by $\psi_i = e - (\Gamma - \lambda \ln p'_i)$. Γ is the void ratio at the critical state at $p' = 1\ kPa$ and λ is the slope of the CSL on a semi-logarithmic scale. $\chi_i = \frac{\chi_{tc}}{1 - \frac{\lambda \chi_{tc}}{M_{tc}}}$ relates maximum dilatancy to ψ_i, with χ_{tc} is that parameter from triaxial compression tests and can be calibrated by plotting the maximum dilatancy measured in drained triaxial tests on dense specimens and the state parameter corresponding to the maximum dilatancy. $M_{i,tc}$ is the M_i in triaxial compression stress state, defined by $M_{i,tc} = M_{tc}\left(1 - \frac{N \chi_i |\psi_i|}{M_{tc}}\right)$ where M_{tc} is the stress ratio (q/p') at the critical state from triaxial compression tests. N is a volumetric coupling coefficient. M_{tc} and N can be calibrated by plotting the relation between the maximum dilatancy and stress ratio measured in drained triaxial tests on dense specimens.

In NorSand, the mean stress at image state, p'_i, is used to control the size of the yield surface. The hardening law of the internal cap is expressed by Equation (2). The negative sign and absolute plastic deviator strain increment show p'_i always decreases at the internal cap, which means the cap always contracts and results in the additional softening.

$$\frac{dp'_i}{p'_i} = -\frac{H}{2}\frac{M_i}{M_{i,tc}}\left|d\varepsilon_q^p\right| \tag{2}$$

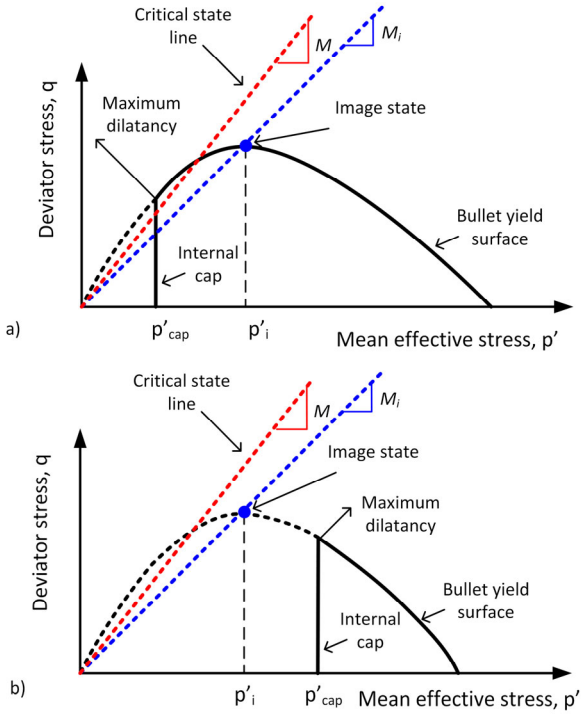

Figure 1. The concept of NorSand model: (a) dense soil, (b) loose soil.

where $d\varepsilon_q^p$ is the plastic deviator strain increment. H is a hardening parameter, $H = H_0 - H_\psi \psi$. ψ is the state parameter, $\psi = e - (\Gamma - \lambda \ln p')$. The details of NorSand and internal cap are available in Jefferies and Been (2015b). NorSand without the internal cap was implemented into UMAT subroutine for Abaqus/Standard by Liu et al. (2025b). NorSand with the internal cap is implemented into UMAT here for following simulations.

The unloading stress paths relatively to bullet yield surface arises when the angle, α, between the gradient of the bullet-shaped yield surface, a_0, and the elastic stress increment, $\Delta\boldsymbol{\sigma}_e$, is greater than 90°. This criterion can be written as Equation (3). In this equation, $a_0 = \frac{\partial f_{bullet}}{\partial \boldsymbol{\sigma}_0}$ is the normal direction of bullet yield surface evaluated at the initial stress state of each increment, $\boldsymbol{\sigma}_0$, $\Delta\boldsymbol{\sigma}_e$ is calculated using the elastic tangential modulus, $\|a_0\|_2$ and $\|\Delta\boldsymbol{\sigma}_e\|_2$ are the Euclidean norm of a_0 and $\Delta\boldsymbol{\sigma}_e$, respectively, and TOL is a suitable tolerance. p' and q decrease in both the unloading stress path and the softening on the bullet yield surface. But the softening on the bullet yield surface produces α less than 90°, which means the value of Equation (3) is greater than $-TOL$. The stress path direction should be checked, and the correct volumetric strain should be given for corresponding stress path.

$$\cos\alpha = \frac{(a_0)^T \Delta\boldsymbol{\sigma}_e}{\|a_0\|_2 \|\Delta\boldsymbol{\sigma}_e\|_2} < -TOL \tag{3}$$

2.2 *Validation by element test simulation*

To validate the developed NorSand with the internal cap UMAT, unloading of triaxial compression tests was simulated. Dabeet (2008) presented the experimental results on Fraser River sand (FRS). The input parameters are summarized in Table 1.

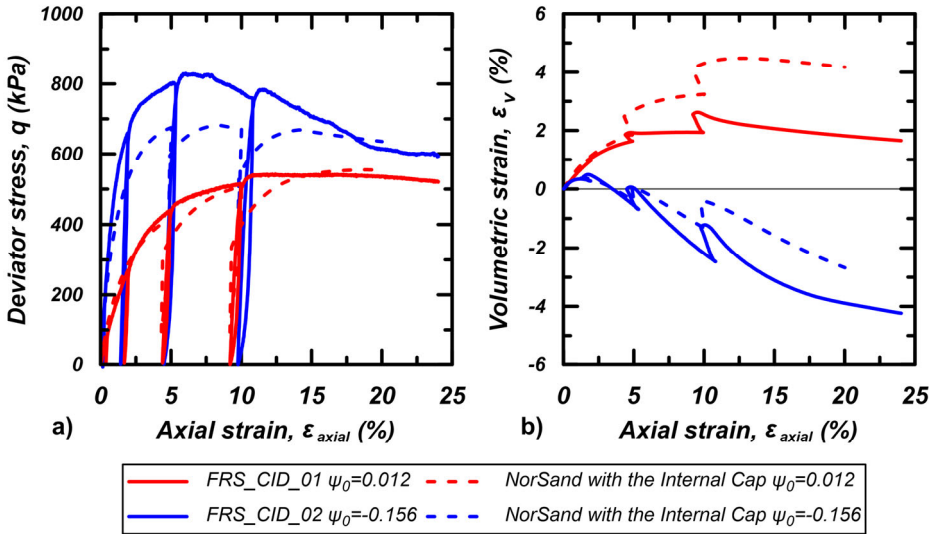

Figure 2. Comparison of simulation results from NorSand UMAT with the internal cap and triaxial compression load-unload-reload data.

In Abaqus, a downward displacement was applied to the top surface of the soil domain in the loading stage, and it was retreated to a smaller displacement in the unloading stage. This process was repeated to simulate the unload-reload loops. The simulation results are compared with experimental data in Figure 2. Two tests were simulated: dense case $\psi_0 = -0.156$, and loose case $\psi_0 = 0.012$. The results show that NorSand with the internal cap is able to capture the unloading behaviour of soils in triaxial compression load-unload-reload cycles. Capturing the contracting volumetric strain in unloading stage for both dense and loose soils is noteworthy.

Table 1. Input parameters for Fraser River sand (Ghafghazi and Shuttle, 2010; Jefferies and Been, 2015).

Parameter	Value
Γ	1.22
λ	0.066
M_{tc}	1.45
N	0.43
χ_{tc}	3.2
H_0	60
H_ψ	280
G (MPa)	$\frac{37.5}{e-0.344} \times (\frac{p'}{100})^{0.5}$
ν	0.2

3 NUMERICAL MODELLING OF CPT TESTS IN SAND

Two CPT chamber tests on Medium Hutcheson Sand conducted by Liu et al. (2025) were simulated to validate the numerical modelling of the CPT. The two versions of NorSand UMAT, i.e. with and without the internal cap, were used to analyze the effect of unloading stress path on CPT.

3.1 *Chamber test setup*

Specimens had a 1.14 m depth and 1.4 m diameter. The chamber is made with 10 mm thick steel, making all walls semi-rigid. The semi-rigid lateral wall results in near-zero lateral displacements.

Tests were performed on Medium Hutcheson (MH) sand; a poorly graded Feldspar- and Quartz-dominated sand (Manmatharajan et al., 2023). The physical properties of MH sand are summarized in Table 2.

Sand specimens were prepared by air pluviation. The sand was deposited into the chamber through a hopper at a constant height and deposition intensity. The hopper moved at a constant rate and followed an S shape curve path during deposition to achieve uniformity. The void ratio was calculated from the weight and volume of the deposited sand. After deposition, the cone was inserted 150 mm into the sample. Then, a vertical stress was applied to the top surface to consolidate the specimen. After consolidation, the cone was pushed into the specimen at a constant 0.005 m/s rate by a hydraulic jack.

Table 2. Physical properties of MH sand (Manmatharajan et al., 2023).

Parameter	Value
G_s	2.7
e_{min}	0.60
e_{max}	0.88
D_{50} (mm)	0.42
D_{10} (mm)	0.22
C_u	2.4

3.2 *Numerical modelling setup*

The chamber tests were simulated in Abaqus/Standard. Figure 3 shows the geometry of the model. The geometry in simulations identical to the chamber tests. The cone radius is 0.01785 m (10 cm^2 cone), and the cone is buried into the soil domain at 0.15 m depth at the beginning.

Arbitrary Lagrangian Eulerian (ALE) formulation was used in an adaptive region to address the large deformations leading to mesh distortions. ALE cannot adjust nodes in the direction constrained by boundary conditions. Therefore, an axisymmetric boundary condition (i.e., no horizontal displacement) cannot be applied to the left surface of soil domain. To solve this issue, a small gap was left between the model and the center axis, but leftward displacement was not allowed at this gap. The adaptive region was defined in the model, as shown in Figure 3. The adaptive region is defined to be perpendicular to the cone tip surface. This definition of the adaptive region helps to have a uniform mesh shape and improves computational stability. The width of adaptive region was 0.1785 m ($5d_c$) and its depth was 0.853 m from top surface (0.6 m below cone tip). ALE mesh smoothing was applied every 3 increments and sweeping number was 5, which means 5 sweeping iterations will be applied in mesh smoothing.

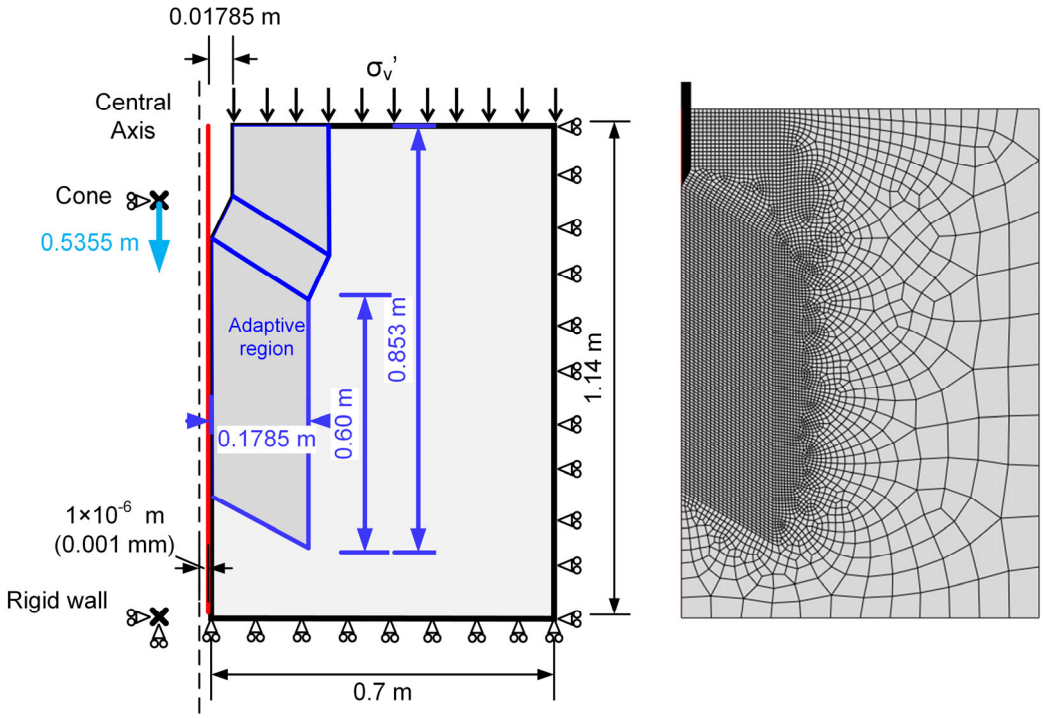

Figure 3. Geometry, mesh and boundary conditions of the CPT model.

The boundary conditions are also presented in Figure 3. The bottom surface of soil domain has no vertical displacement. The horizontal direction displacement was constraint on the right hand side boundary because the chamber wall is semi-rigid. A vertical stress was applied to the top surface of soil domain. A uniform stress state with the vertical stress and K_0 was applied within soil domain. Because the cone has a much higher stiffness than the soil, a rigid body constraint was applied to the cone. This setup also improves the stability of numerical modelling. A 0.5355m ($15d_c$) downward displacement was applied on the cone at a rate of 0.005 m/s.

Even though the simulated cases are drained, the coupled hydromechanical analysis in Abaqus/Standard, soils step, was used. To achieve drained conditions, the permeability of the soil was input as 1 m/s. A flux boundary condition was applied to the top surface of soil domain. CAX4P elements were used in the soil domain and CAX4 elements were used in the cone. In the adaptive region, the width and length of elements are 0.006 m and 0.009 m, respectively. Sensitivity analysis on mesh size showed that the further reduction of mesh size has no effect on simulation results. In other regions, a coarser mesh was used.

Table 3. NorSand parameters for MH sand (Mozaffari et al., 2022).

Parameter	Value
Γ	0.965
λ	0.038
M_{tc}	1.25
N	0.2
χ_{tc}	6.0
H_0	300
H_ψ	2100
G (MPa)	$82.7 \times \frac{(2.2-e)^2}{1+e}(\frac{p}{100})^{0.5}$
ν	0.2

The calibrated NorSand parameters for MH sand are listed in Table 3. The shear modulus is measured from bender element tests. 1/10 of that value was used in this paper, consistent with that recommended by Ghafghazi (2025). Other parameters in Table 3 were not changed.

The coefficient of friction, μ, on cone-soil interface is required in CPT simulation. Zhao et al. (2025) conducted friction cell tests to test frictional coefficient between CPT and MH sand. Their results report that μ is 0.22 for dense case and 0.17 for loose case. In this paper, the average value of 0.2 was used.

Two chamber tests were simulated for validation. The stress state, void ratio, and state parameter are summarized in Table 4. Both cases are dense, one medium dense ($\psi_0 = -0.096$), and the other dense ($\psi_0 = -0.226$).

Table 4. Summary of simulated chamber tests (Liu et al., 2025a).

Chamber test No.	σ_v'	K_0	e	ψ_0
4	300	0.348	0.675	-0.096
5	100	0.308	0.588	-0.226

3.3 *Numerical Results*

Figure 4 compares simulation results and chamber test data. The comparison shows that tip resistance from simulations agrees well with chamber test data. For $\psi_0 = -0.226$, the tip resistance from simulation (11.8 MPa for NorSand without the internal cap) is less than the chamber test data (14.0 MPa). For $\psi_0 = -0.096$, the tip resistance is 1.6 MPa higher for simulation (9.8 MPa for NorSand without the internal cap) than chamber test (8.2 MPa). The simulated sleeve friction is higher than chamber test data. For $\psi_0 = -0.226$, the sleeve friction from NorSand without the internal cap is 410.2 kPa, but the chamber test data is 30.2 kPa. For $\psi_0 = -0.096$, the sleeve friction from NorSand without the internal cap is 344.4 kPa, but the chamber test data is 20.9 kPa.

The simulation results from NorSand without internal cap are also compared with that from NorSand with internal cap in Figure 4. The tip resistance slightly increases for the case with $\psi_0 = -0.226$ when internal cap is included (i.e., 13.3MPa for NorSand with internal cap, 11.9 MPa for NorSand without internal cap). The change is negligible for the case with $\psi_0 = -0.096$ (i.e., 10.1 MPa for NorSand with internal cap, 9.8 MPa

for NorSand without internal cap). However, the internal cap has a significant effect on sleeve friction. The sleeve friction is reduced because of the internal cap for both $\psi_0 = -0.096$ and $\psi_0 = -0.226$. For the case with $\psi_0 = -0.096$, the sleeve friction decreases from 344.4 kPa to 222.7 kPa when internal cap is included in NorSand (i.e., 35.3% reduction). For the case with $\psi_0 = -0.226$, the sleeve friction decreases from 410.2 kPa to 236.0 kPa when internal cap is included in NorSand (i.e., 42.3% reduction). The inclusion of the internal cap in NorSand improves the comparison between the simulation results and the chamber tests sleeve friction. This is because, the internal cap affects the stress response in the region behind the cone.

4 DISCUSSION

Figure 5(a) shows the stress paths during penetration at a point 0.0714 m ($2d_c$) from the center. The stress variation during penetration can be generally divided into two stages, loading and unloading. In the loading stage, both p' and q increase and the slope of $q - p'$ curve is almost constant. The slope for $\psi_0 = -0.226$ is higher than that for $\psi_0 = -0.096$, which means the stress state increases faster in the denser case. This faster increase is contributed from the larger dilatancy in the denser case. The stress state keeps increasing until the stress state approaches the maximum value. For $\psi_0 = -0.226$, NorSand with the internal cap produces a slightly larger maximum value than NorSand without the internal cap, which results in a higher tip resistance. For $\psi_0 = -0.096$, these two models produce almost the same stress paths, so the tip resistances are the same for these models. After approaching the maximum values, both p' and q start to decrease. In this case, α is greater than 90°, which means the stress path is inward relatively to the bullet-shaped yield surface and the soil starts to be unloaded. The unloading stress path starts after the tip passes but before the cone shoulder passes. For NorSand without the internal cap, p' and q decrease at same slope to loading stage. However, when the internal cap is included, p' and q decrease with a steeper slope and this results in a lower stress state than NorSand without the internal cap. The lower stress state contributes to the lower sleeve friction when the internal cap is included.

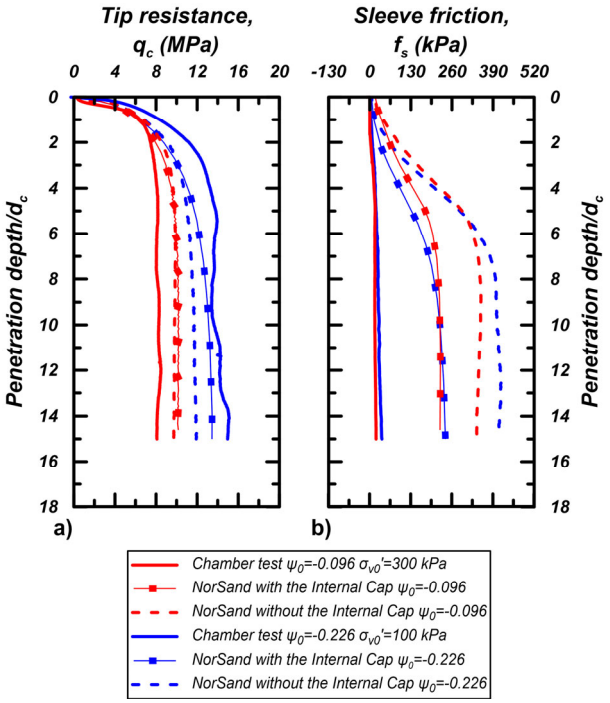

Figure 4. Comparison of CPT simulation results and chamber test data: (a) tip resistance q_c, (b) sleeve friction f_s.

Figure 5(b) shows the variation of p_i' during penetration, which presents the movement of yield surface. During the loading stage, p_i' increases with increase in p', so the model is hardening. p_i' reaches its maximum value when the cone shoulder arrives. When the unloading starts, for NorSand without the internal cap, p_i' remains constant, meaning the soil response is elastic. However, for NorSand with the internal cap, p_i' decreases with the decrease in p'. This means the unloading stress path crosses the internal cap and produces the additional plastic response. The additional plastic response on the internal cap due to unloading contributes to the faster decrease in the stress state, and further reduction in the sleeve friction. This additional softening is more evident in the denser case ($\psi_0 = -0.226$).

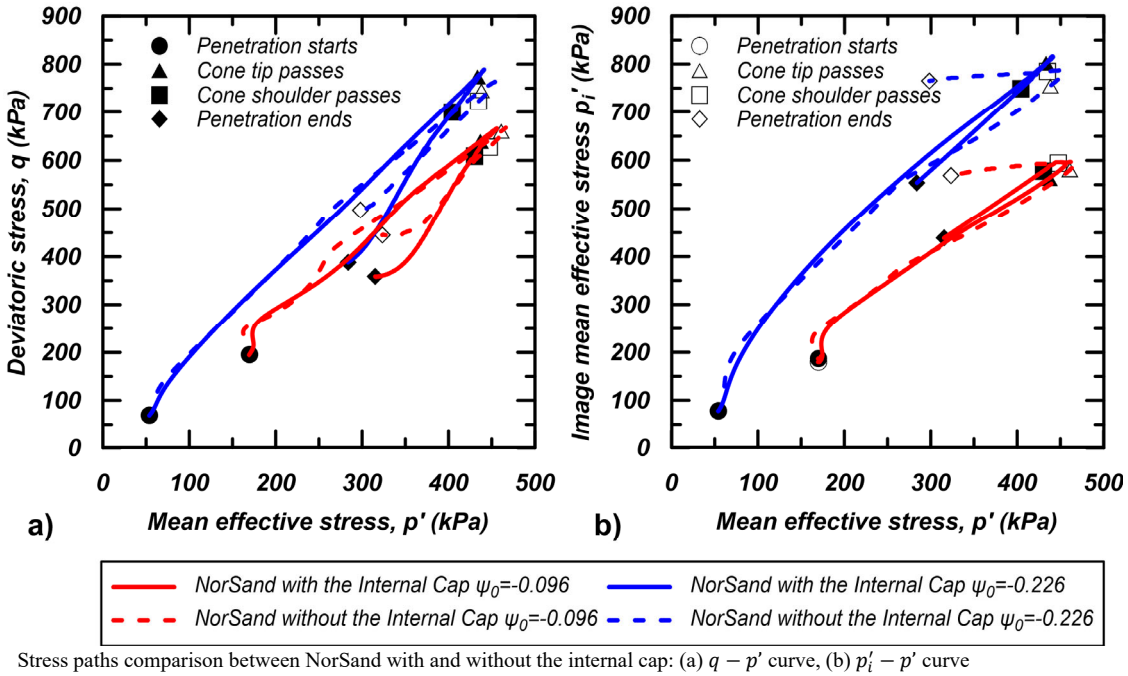

Figure 5. Stress paths comparison between NorSand with and without the internal cap: (a) $q - p'$ curve, (b) $p_i' - p'$ curve

5 CONCLUSIONS

CPT is the primary tool in geotechnical engineering for estimating in-situ soil properties. Past research shows that both loading and unloading stress paths occur around the cone. However, in most existing numerical models of the CPT, the unloading behind the cone has not been simulated well. This is because the unloading is either ignored or assumed as elastic in the constitutive models used in these simulations.

NorSand with the internal cap was implemented into the UMAT subroutine of Abaqus/Standard. The UMAT was validated by simulating triaxial unloading. The results showed that the internal cap can capture soil behaviour in unloading conditions well.

Two CPT chamber tests in a poorly graded dry sand were simulated in Abaqus/Standard using NorSand with and without the internal cap. The simulation results showed tip resistance from simulations have good comparison with chamber test data, but the sleeve friction is higher than that from chamber tests. The results also showed that the inclusion of the internal cap in NorSand reduces the sleeve friction. The stress variation during penetration was analyzed. It was shown that the unloading stress path crossing the internal cap can reduce the stress state when the cone shoulder passes. It subsequently reduces the sleeve friction. The inclusion of internal cap and unloading behaviour can improve the estimated values of both tip resistance and sleeve friction, leading to better interpretation methods stemming from computational models.

6 ACKNOWLEDGEMENTS

Authors express their gratitude to Vale Brazil and Office of the VP International (OVPI) at University of Toronto for Toronto-Melbourne joint training program which enabled this work. The collaboration with Mr. Zhenyu Liu and Mr. Wyatt Handspiker is also greatly appreciated.

7 REFERENCES

Ayala, J., Martinelli, M., Reid, D., and Fourie, A., 2023. Cone resistance and soil state of tailing sand deposits using the Material Point Method. In: L. Zdravkovic, S. Kontoe, D. Taborda and A. Tsiampousi, eds. *10th European Conference on Numerical Methods in Geotechnical Engineering*. London, UK.

Dabeet, A.E., 2008. *A Practical Model for Load-Unload-Reload Cycles on Sand*. The University of British Columbia.

Ghafghazi, M., 2025. Reply to the discussion on our paper "Material-specific interpretation of the state parameter from drained cone penetration test" by Mohammad RazaviNasab, Katia Boschi, and Marcos Arroyo. *Canadian Geotechnical Journal*, 62, pp.1–5.

Ghafghazi, M., and Shuttle, D., 2008. Interpretation of sand state from cone penetration resistance. *Géotechnique*, 58(8), pp.623–634.

Ghafghazi, M., and Shuttle, D., 2010. Interpretation of the in situ density from seismic CPT in Fraser River sand. In: P. Robertson and P. Mayne, eds. *2nd International Symposium on Cone Penetration Testing*. Huntington Beach, USA.

Handspiker, W., and Ghafghazi, M., 2024. A Review of the NorSand Constitutive Model's Capabilities in Representing Common Loading Modes in Soil Mechanics. In: T. Matthew Evans, N. Stark and S. Chang, eds. *Geo-Congress 2024: Geotechnical Site and Soil Characterization*. Vancouver, Canada. pp.294–303.

Jefferies, M., 1997. Plastic work and isotropic softening in unloading. *Géotechnique*, 47(5), pp.1037–1042.

Jefferies, M., and Been, K., 2015. *Soil Liquefaction: A Critical State Approach*. Second edn. Boca Raton, USA: CRC Press.

Jefferies, M.G., 1993. Nor-Sand: a simple critical state model for sand. *Géotechnique*, 43(1), pp.91–103.

Liu, W., Talesnick, M., and Ghafghazi, M., 2025a. Full State of Stress and Strain at a Point near the Cone during Penetration Tests in Sand. *Journal of Geotechnical and Geoenvironmental Engineering*, 151(7), p.4025056.

Liu, Z., Chow, S.H., Tian, Y., and Ghafghazi, M., 2025b. *Three-dimensional numerical modelling of drained uplift capacity of rectangular plate anchors using NorSand*. [Unpublished manuscript].

Liu, Z., Chow, S.H., Wu, X., Ghafghazi, M., and Tian, Y., 2024. Numerical investigation of horizontal plate anchor capacity in dilating sand. In: T. Powell, ed. *9th International Offshore Site Investigation and Geotechnics Conference (OSIG 2023)*. London, UK: Society for Underwater Technology. pp.1582–1589.

Manmatharajan, M.V., Gill, S., Liu, W., Ingabire, E.-P., Sy, A., and Ghafghazi, M., 2023. Effect of particle size and particle size distribution on critical state loci of granular soils. *Canadian Geotechnical Journal*, 60(8), pp.1117–1131.

Martinelli, M., Remmerswaal, G., and Reid, D., 2024. State parameter predictions based on cone penetration test simulated with MPM: an application to tailing deposits. *Géotechnique Letters*, 14(4), pp.1–27.

Moug, D.M., Boulanger, R.W., DeJong, J.T., and Jaeger, R.A., 2019. Axisymmetric Simulations of Cone Penetration in Saturated Clay. *Journal of Geotechnical and Geoenvironmental Engineering*, 145(4), p.4019008.

Mozaffari, M., and Ghafghazi, M., 2023. Material-specific interpretation of the state parameter from drained cone penetration test. *Canadian Geotechnical Journal*, 61(12), pp.2858–2872.

Mozaffari, M., Liu, W., and Ghafghazi, M., 2022. Influence of specimen nonuniformity and end restraint conditions on drained triaxial compression test results in sand. *Canadian Geotechnical Journal*, 59(8), pp.1414–1426.

Yi, J.T., Goh, S.H., Lee, F.H., and Randolph, M.F., 2012. A numerical study of cone penetration in fine-grained soils allowing for consolidation effects. *Géotechnique*, 62(8), pp.707–719.

Yu, H.S., and Houlsby, G.T., 1991. Finite cavity expansion in dilatant soils: loading analysis. *Géotechnique*, 41(2), pp.173–183.

Zhao, H., Wu, X., Mcclenaghan, A., Cross, R., Sharp, J., and Ghafghazi, M., 2025. Direct Measurement of CPT Sleeve-Sand Interface Coefficient of Friction. In: K. Bannister, D. Kurz and A. Jianfar, eds. *78th Canadian Geotechnical Conference (GeoManitoba 2025)*. Manitoba, Canada.